

Three-dimensional visualisation of coronary sinus ostium from the inside right atrium perspective

Rafał Młynarski¹, Agnieszka Młynarska², Krzysztof S. Gołba³, Maciej Sosnowski⁴

¹Department of Electrophysiology, Upper Silesian Medical Centre, Katowice, Poland

²Department of Internal Nursing, Chair of Internal Medicine, Medical University of Silesia, Katowice, Poland

³Department of Electrophysiology and Heart Failure, School of Health Sciences, Medical University of Silesia, Katowice, Poland

⁴3rd Division of Cardiology, Medical University of Silesia, Katowice, Poland

Abstract

Background: There is no *in vivo* method of coronary sinus visualisation from the right atrium perspective.

Aim: The objective of the study was to create a cardiac computed tomography (CT) angiography-based method of visualising the coronary sinus ostium and the Thebesian valve from the inside right atrium perspective.

Methods: In 78 consecutive patients, a cardiac CT angiography (Aquilion 64, Toshiba) with retrospective gating (slice 0.5 mm) was performed. Raw data were reconstructed on Vitrea 2 workstations (Vital Images). In order to create the three-dimensional (3D) coronary sinus visualisation from the “inside view” perspective, patented “Fly Through” algorithms were used, and the anatomical positions on the multiplanar reconstruction images were marked. A dedicated, Likert-based five-point scale was developed and used to evaluate the quality of the visualisations.

Results: The average quality of the visualisations of the coronary sinus ostium in two-dimensional multiplanar reconstruction images was good (4.17 ± 0.85 points) and was clinically interpretable in all cases. The image quality of the “inside view” 3D images was 3.61 ± 1.12 points. In 57.7% of cases we obtained high scores (4 and 5 points). The main diameter was 10.72 ± 2.48 mm, and the entrance angle of the coronary sinus into the right atrium was $103.76 \pm 10.71^\circ$.

Conclusions: Cardiac CT angiography is a useful method that permits the coronary sinus ostium and Thebesian valve to be visualised *in vivo* from the inside of the right atrium in a comparable manner.

Key words: coronary venous system, Thebesian valve, cardiac computed tomography angiography, three-dimensional

Kardiol Pol 2018; 76, 3: 536–541

INTRODUCTION

Cannulation of the coronary sinus (CS) is a standard feature in selected electrophysiology procedures, including during the implantation of cardiac resynchronisation therapy devices. Sometimes, anatomical relationships cause cannulation to be more difficult or even impossible [1, 2]. Many methods have been tested to visualise the coronary venous system, including cardiac computed tomography (CT) angiography, cardiac magnetic resonance, echocardiography, or even electroanatomical mapping [3–5]. Each of those techniques has both advantages and disadvantages due to their technical specifications. Comparisons of the technical possibilities show that the most advanced technical image specification

can be found in multi-slice CT scanners. They also offer the possibility to create the three-dimensional (3D)-like images.

However, in the literature, there is a lack of anatomical 3D anatomic-like images of the CS ostium from the right atrium perspective, which can be valuable for the electrophysiology procedures mentioned earlier.

The objective of the study was to create a CT-based method for visualising the CS ostium and the Thebesian valve from the inside right atrium perspective.

METHODS

Seventy-eight consecutive patients (average age 70.3 ± 13.94 years; 41 women) who had been qualified for cardiac

Address for correspondence:

Rafał Młynarski, MD, PhD, Department of Electrophysiology, Upper Silesian Medical Centre, ul. Ziolowa 45, 40–635 Katowice, Poland, e-mail: joker@mp.pl

Received: 24.09.2017

Accepted: 23.11.2017

Available as AoP: 08.12.2017

Kardiologia Polska Copyright © Polskie Towarzystwo Kardiologiczne 2018

CT angiography were included into this study. Cardiac CT angiography was originally performed due to a suspicion of coronary artery disease (typical indications). Computed tomography was performed using a 64-slice scanner (Aquilion 64, Toshiba Medical, Japan). Exclusion criteria were as follows: atrial fibrillation or other heart rhythm disorders, renal insufficiency (serum creatinine > 1.2 mg/dL), hyperthyroidism, a known allergy to non-ionic contrast agents, or a previously implanted pacemaker with unipolar leads.

A local Bioethical Committee approved this study. All of the participants gave their signed informed consent. The study protocol conformed to the version of the Helsinki Convention that was valid at the time the study was designed.

Computed tomography protocol

Scanning with retrospective electrocardiography (ECG)-gating was performed during a breath hold using 64 slices with a collimated slice thickness of 0.5 mm using the standard protocol for coronary arteries.

The helical pitch was 12.8 (best mode) and the rotation time was 0.4 s. The tube voltage was strictly dependent on the patient's body mass index (BMI): for BMI < 23.9 kg/m² it was 120 kV at 330 mA, for BMI 24.0–29.9 kg/m² it was 135 kV at 380 mA, and for BMI > 30.0 kg/m² it was 135 kV at 430 mA. We used a pre-selected region of interest (ROI) in the descending aorta. Triggering started at 180 Hounsfield units. About 80–100 mL of non-ionic contrast agent (iopromide 768.86 mg/mL, Ultravist 370, Bayer Schering, Germany) was given to each patient. Sometimes, when the heart rhythm was higher than 65 bpm, metoprolol succinate (5–10 mg) was administered intravenously unless contraindicated. If the expected heart rhythm (65 bpm) slowing did not occur, the patient was excluded from the study. Sublingual application of nitroglycerine was not used in this study.

Post-processing

Reconstructions of the data were performed on Vitrea 2 workstations (Vital Images, USA). To reconstruct the 3D CS and the great cardiac vein from the inside view, a coronary artery algorithm was used. In the gallery window, a pre-set called "Fly Through" was used. The zoom function and rotating 3D images were used simultaneously through the centre of the view. To confirm the anatomical positions, multiplanar two-dimensional (2D) reconstructions (MPR) were used and in some cases 2D/3D markers (arrows) were added as well.

The aims for the visualisations of the coronary venous system were as follows:

- visualisation of the CS ostium from the right atrium perspective;
- visualisation of the Thebesian valve (always confirmed on the MPR) from the right atrium perspective.

Images were graded by two experts trained in multi-slice CT and experienced in the visualisation of the coronary venous

Table 1. Characteristics of the patients

	Mean ± SD
Ejection fraction [%]	65.49 ± 12.46
End-diastolic volume [mL]	131.47 ± 52.18
End-systolic volume [mL]	49.79 ± 37.19
Stroke volume [mL]	86.45 ± 28.14
Cardiac output [L/min]	5.06 ± 1.49
Myocardial mass [g]	169.83 ± 55.28
Myocardial volume [mL]	159.72 ± 53.46

Data are shown as mean ± standard deviation (SD).

system. A dedicated Likert-based scale was created and used to evaluate the quality of the visualisations. In the five-point scale, one point indicates a highly schematic visualisation of the CS ostium and five indicates the best quality with a complete clinical input.

Statistical analysis

All the calculations were performed using the Polish version of Statistica (Stat Soft, Tulsa, Oklahoma, US). Continuous data were presented as mean ± standard deviation. The Student's t-test was used to compare the quantitative data with a normal distribution, and the χ^2 test was used for the nonparametric data. In order to assess whether the analysed parameters were predictors of the dependent variables, multiple regression analysis using the stepwise method was used. Results were recognised as statistically significant at $p < 0.05$.

Reproducibility of the phase determination was evaluated using the Bland-Altman method. The calculation of the inter-rater agreement coefficient kappa was performed by using MedCalc (Ostend, Belgium) statistical software.

RESULTS

The characteristics of the included patients are presented in Table 1. Arterial hypertension (84.6%), hypercholesterolaemia (70.5%), and family history of cardiovascular diseases (53.8%) were the most prevalent risk factors. Diabetes (33.3%) and smoking (28.2%) were also observed in the included patients.

The CS ostium was measured using 2D MPR images in all of the patients — average quality of the visualisations was quite good (4.17 ± 0.85) and in 100% was useful for clinical analysis (Fig. 1, left panel). The main diameter (diameter between the farthest points put in the opposite walls of the vessel) was evaluated as 10.72 ± 2.48 mm in the entire population. It was significantly greater ($p = 0.0113$) in the men (11.46 ± 2.66 mm) compared to the women (10.05 ± 2.13 mm). The angle of entry into the CS into the right atrium was $103.76 \pm 10.71^\circ$; for the women it was $104.78 \pm 9.99^\circ$ and for the men $102.63 \pm 11.49^\circ$, although in this case the differences were not statistically significant.

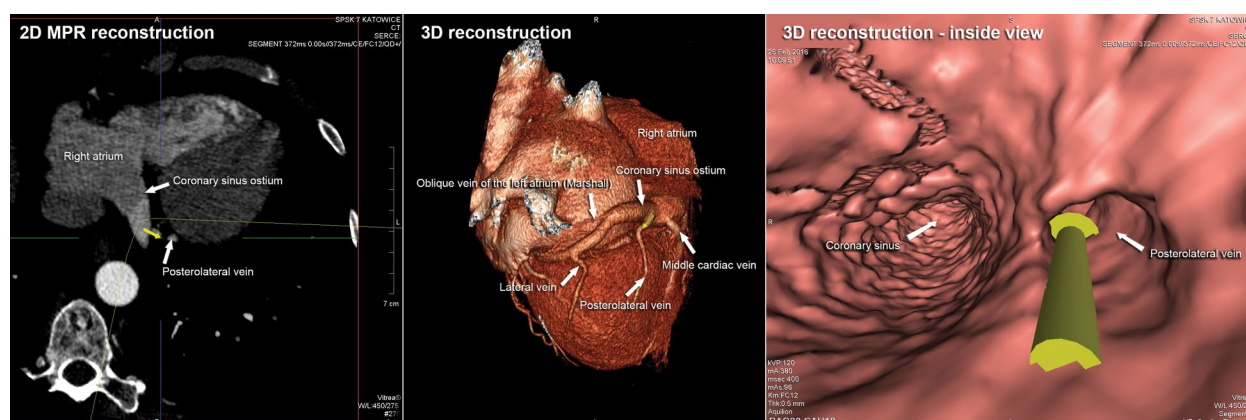


Figure 1. Different types of visualisations of the coronary sinus ostium: two-dimensional multi-planar reconstruction, three-dimensional (3D) volume rendering and the newly created 3D inside view. Yellow 3D arrow is used to mark the position of the posterolateral vein on each reconstruction

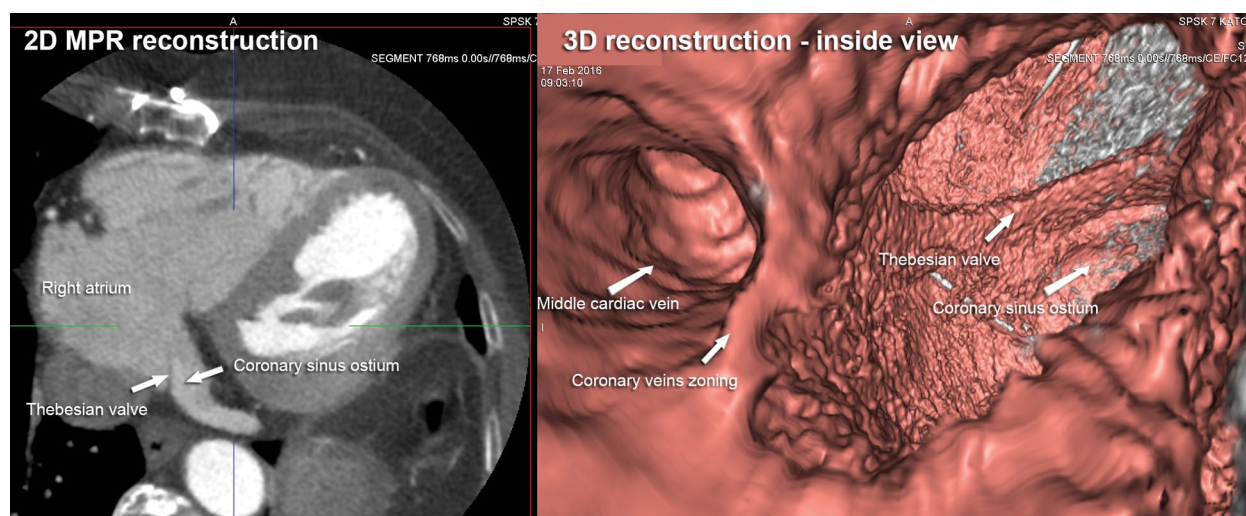


Figure 2. Visualisation of the Thebesian valve using two-dimensional multi-planar reconstruction and the newly created three-dimensional “inside view”

3D visualisation from the inside view

The different types of CS ostium visualisation in cardiac CT angiography are presented in Figure 1, including a 2D MPR, a 3D volume rendering, and the newly created 3D “inside view”. In 94.8% of images, a complete convergence between the different techniques was observed. We were able to visualise the Thebesian valve as a guard of the CS in 41.02% of the patients using our 3D “inside view” technique.

The visualisation of CS ostium including the Thebesian valve using 2D MPR and the newly created 3D inside view is presented in Figure 2. Examples of the newly created 3D “inside view” of the CS and coronary veins are presented in Figure 3.

3D visualisation from the inside view — the quality

The quality of the visualisation of the 3D images was evaluated as 3.61 ± 1.12 . In 57.7% of cases, we obtained high scores (4 and 5 points). Images were clinically interpretable in all cases. We also performed gender-dependent analysis: in women, the average quality was 3.71 ± 1.10 and was not significantly better than in the men — 3.51 ± 1.14 ($p = 0.804$).

Regression models

A multiple regression model in which the predictors were the average CS diameter, the angle of the entry of the CS into the right atrium, and the CS ostium diameter, and the dependent variable was the quality 3D “inside view” images, was statisti-

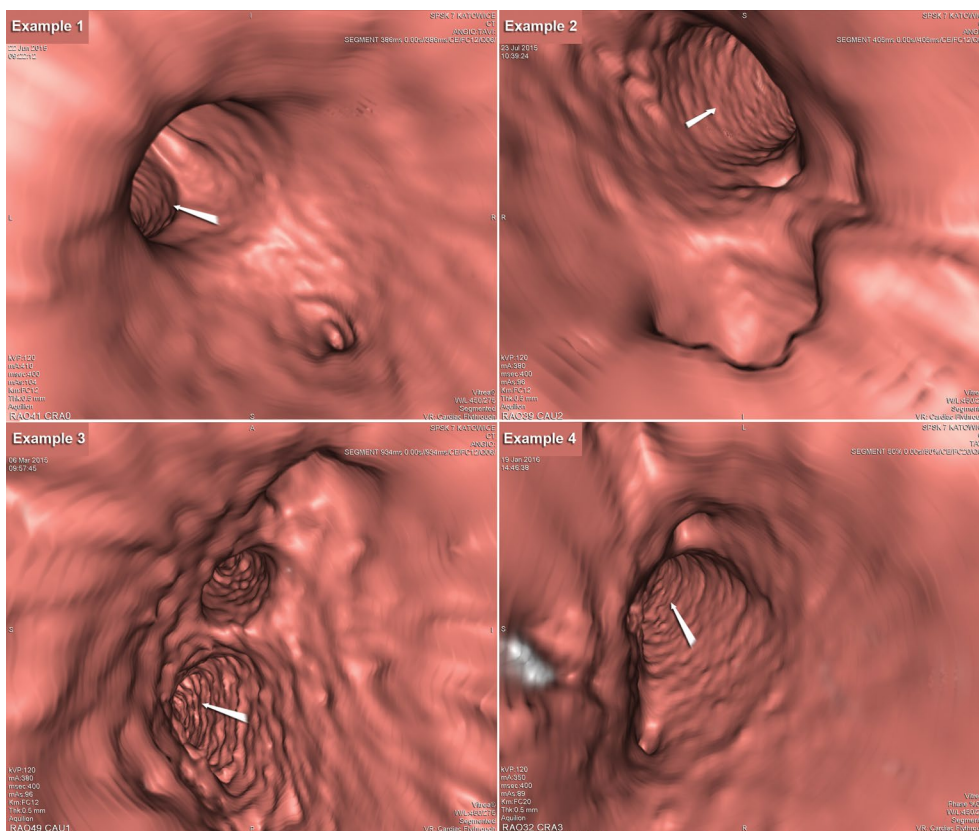


Figure 3. Examples of the newly created three-dimensional inside view of the coronary sinus and coronary veins

cally significant and explained 8.6% of the observed variance in the dependent variable ($p = 0.0096$; $R^2 = 0.0861$). The analysis showed that the average CS diameter ($p = 0.0096$) is an important predictor of the dependent variable.

A multiple regression model in which the predictors were stroke volume, cardiac output, ejection fraction, and end systolic volume, and the dependent variable was the quality of the 3D “inside view” images, was statistically significant and explained 12.7% of the observed variance in the dependent variable ($p = 0.0008$; $R^2 = 0.1273$). The analysis showed that stroke volume ($p = 0.0008$) is an important predictor of the dependent variable.

Agreement between observers

There was a very good agreement between observers in the evaluation of the quality CS “inside view evaluation” (95% confidence interval [CI] 0.841–0.979, inter-rater agreement kappa 0.910). There were similar results in the repeated evaluation of the score by the same observer (95% CI 0.955–1.000; kappa 0.985).

DISCUSSION

The valve of the CS, which is sometimes called the Thebesian valve, is a semi-circular fold of the lining membrane of the right atrium, at the orifice of the CS [1]. It is situated at the base of the

inferior vena cava. The valve may vary in size or be completely absent. Holda et al. [1], after exact evaluation of 273 autopsied human heart valves, differentiated according to their shape, found five types of valve: remnant, semilunar, fold, cord, and mesh and fenestrated. Another qualification of Thebesian valve based on 2D CT imaging was proposed by Mlynarski et al. [6]

Visualisation of the coronary venous system was underestimated for years mostly due to its lack of clinical usefulness. However, because of some electrophysiology procedures like cardiac resynchronisation therapy, percutaneous mitral annuloplasty, or ablation, its visualisation has become very important due to the necessity of CS cannulation [7–9]. While 20 years ago most of the papers about the visualisation of the coronary veins reported post mortem examinations, today electrophysiologists require *in vivo* imaging [10].

The rapid development of *in vivo* imaging techniques has been accompanied by true advances. Visualisation of the coronary venous system began in 2001 when Gerber et al. [11] confirmed the possibility of visualising the coronary veins using electron beam CT.

During subsequent years, papers from different centres described the anatomy of the coronary venous system, precisely defined the different anatomical variants, and showed the clinical usefulness of the 3D images in multi-layer cardiac CT [12–16].

In terms of clinical usefulness, some schemes for using visualisation to support cardiac resynchronisation were also developed — one that was proposed by our team in which we created a scheme for visualisation in CT that was comparable to fluoroscopy imaging was published in 2009 [17].

Nevertheless, most of those papers described the anatomy of the venous system using 3D visualisation from the outside perspective, and none of them visualised the anatomy from the inside view of the right atrium. Although algorithms to virtually “enter” the blood vessel have existed for years, they have not been used to visualise the coronary venous system. Hence, the objective of this research was to create an “inside view” of the CS and the proximal part of the coronary venous system using “Fly Through” algorithms. We documented that in more than 50% of patients, the quality of these images was at least good and was fully acceptable for clinical evaluation. Using our “inside view” method, we were also able to visualise the Thebesian valve, which is an anatomical guard of the coronary sinus from the right atrium [18]. In some individuals, the valve is degenerated or does not exist, and very rarely is it so big or porous that it can influence coronary circulation and be a real problem during CS cannulation [19, 20]. However, if we compare the average occurrence of this valve with other researchers, our instances of its occurrence are slightly lower [21]. We believe that this may be caused by a lack of the visualisation of very small Thebesian valves. We think that the resolution of the proposed method may be too low in such cases. This reinforces the necessity to always confirm clinical anatomical discoveries. In our paper we also try to find factors that can influence the quality of 3D “inside view” images. The analysis showed that the average coronary sinus diameter ($p = 0.0239$) and stroke volume are important predictors of the quality of 3D images.

To our knowledge, there have been no reports similar to this research on cardiac CT. However, there is one description of using 3D echocardiography to cannulate the CS. Mahmoud et al. [22] presented a case of a 78-year-old patient in whom a CARILLON, which is a device for percutaneous mitral annuloplasty, was implanted. The use of fluoroscopy and 3D transoesophageal echocardiography for CS cannulation was unsuccessful. The authors created an anatomically oriented enface view of the interatrial septum from the right atrial perspective, identified the CS ostium, and cannulated it successfully. The authors concluded that real-time 3D transoesophageal echocardiography can be used to guide CS cannulation because it provides an anatomically oriented and informative enface view of the CS ostium. The paper presented the practical use of 3D techniques. However, the authors used echocardiography, whose image quality including resolution is worse than in cardiac CT, although echocardiographic images are available in real time.

It is worth mentioning that another valve that sometimes causes problems with target coronary vein cannulation is the Vieussens valve — this is a valve between the CS and the great cardiac vein. It is clinically important because it can cause obstruction for electrophysiology catheters in as many as 20% of cases [23–25]. In the presented CT-based study the Vieussens valve was not observed.

We believe that the continuous development in the 3D techniques that permit the CS to be visualised from the right atrium perspective along with CT and echocardiography can support CS cannulation in selected cases.

Limitations of the study

The aim of the study was to create methods to visualise the CS and the Thebesian valve from the right atrium perspective — it is mostly a descriptive anatomical study. The presented study analysed only the presence of the valve itself without distinguishing different types. Currently, the clinical usefulness of the proposed techniques is limited to very rare cases in which a previous problem with the CS ostium occurred. The authors believe that this can change in the near future due to the rapid development of modern CT techniques.

CONCLUSIONS

Cardiac CT angiography appears to be a useful method that permits the CS ostium and the Thebesian valve to be visualised *in vivo* from the inside of the right atrium in a comparable manner. The average CS diameter and stroke volume are predictors of high-quality 3D “inside view” images.

Conflict of interest: none declared

References

1. Hołda MK, Klimek-Piotrowska W, Koziej M, et al. Anatomical variations of the coronary sinus valve (Thebesian valve): implications for electrocardiological procedures. *Eurpace*. 2015; 17(6): 921–927, doi: [10.1093/europace/euu397](https://doi.org/10.1093/europace/euu397), indexed in Pubmed: [25767087](https://pubmed.ncbi.nlm.nih.gov/25767087/).
2. Gokhroo RK, Bisht DS, Padmanabhan D, et al. Coronary sinus anatomy: Ajmer Working Group Classification. *J Invasive Cardiol*. 2014; 26(2): 71–74, indexed in Pubmed: [24486664](https://pubmed.ncbi.nlm.nih.gov/24486664/).
3. Młynarski R, Młynarska A, Sosnowski M. Anatomical variants of left circumflex artery, coronary sinus and mitral valve can determine safety of percutaneous mitral annuloplasty. *Cardiol J*. 2013; 20(3): 235–240, doi: [10.5603/CJ.2013.0067](https://doi.org/10.5603/CJ.2013.0067), indexed in Pubmed: [23788296](https://pubmed.ncbi.nlm.nih.gov/23788296/).
4. Nguyễn UC, Mafi-Rad M, Aben JP, et al. A novel approach for left ventricular lead placement in cardiac resynchronization therapy: Intraprocedural integration of coronary venous electroanatomic mapping with delayed enhancement cardiac magnetic resonance imaging. *Heart Rhythm*. 2017; 14(1): 110–119, doi: [10.1016/j.hrthm.2016.09.015](https://doi.org/10.1016/j.hrthm.2016.09.015), indexed in Pubmed: [27663606](https://pubmed.ncbi.nlm.nih.gov/27663606/).
5. Habib A, Lachman N, Christensen KN, et al. The anatomy of the coronary sinus venous system for the cardiac electrophysiologist. *Eurpace*. 2009; 11 Suppl 5: v15–v21, doi: [10.1093/europace/eup270](https://doi.org/10.1093/europace/eup270), indexed in Pubmed: [19861386](https://pubmed.ncbi.nlm.nih.gov/19861386/).
6. Młynarski R, Młynarska A, Tendera M, et al. Coronary sinus ostium: the key structure in the heart's anatomy from the electro-

- physiologist's point of view. *Heart Vessels*. 2011; 26(4): 449–456, doi: [10.1007/s00380-010-0075-3](https://doi.org/10.1007/s00380-010-0075-3), indexed in Pubmed: [21240507](https://pubmed.ncbi.nlm.nih.gov/21240507/).
7. Sperzel J, Reiner C, Schwarz T, et al. Left ventricular leads used in cardiac resynchronization therapy for heart failure patients. *Herzschrittmacherther Elektrophysiol*. 2001; 12(4): 195–203, doi: [10.1007/s003990170004](https://doi.org/10.1007/s003990170004), indexed in Pubmed: [27432389](https://pubmed.ncbi.nlm.nih.gov/27432389/).
 8. Feldman T, Young A. Percutaneous approaches to valve repair for mitral regurgitation. *J Am Coll Cardiol*. 2014; 63(20): 2057–2068, doi: [10.1016/j.jacc.2014.01.039](https://doi.org/10.1016/j.jacc.2014.01.039), indexed in Pubmed: [24583296](https://pubmed.ncbi.nlm.nih.gov/24583296/).
 9. Huang SK, Graham AR, Bharati S, et al. Short- and long-term effects of transcatheter ablation of the coronary sinus by radiofrequency energy. *Circulation*. 1988; 78(2): 416–427, doi: [10.1161/01.cir.78.2.416](https://doi.org/10.1161/01.cir.78.2.416), indexed in Pubmed: [3396178](https://pubmed.ncbi.nlm.nih.gov/3396178/).
 10. DeSimone CV, De Simone CV, Noheria A, et al. Myocardium of the superior vena cava, coronary sinus, vein of Marshall, and the pulmonary vein ostia: gross anatomic studies in 620 hearts. *J Cardiovasc Electrophysiol*. 2012; 23(12): 1304–1309, doi: [10.1111/j.1540-8167.2012.02403.x](https://doi.org/10.1111/j.1540-8167.2012.02403.x), indexed in Pubmed: [22830489](https://pubmed.ncbi.nlm.nih.gov/22830489/).
 11. Gerber TC, Sheedy PF, Bell MR, et al. Evaluation of the coronary venous system using electron beam computed tomography. *Int J Cardiovasc Imaging*. 2001; 17(1): 65–75, indexed in Pubmed: [11495511](https://pubmed.ncbi.nlm.nih.gov/11495511/).
 12. Jongbloed MRM, Lamb HJ, Bax JJ, et al. Noninvasive visualization of the cardiac venous system using multislice computed tomography. *J Am Coll Cardiol*. 2005; 45(5): 749–753, doi: [10.1016/j.jacc.2004.11.035](https://doi.org/10.1016/j.jacc.2004.11.035), indexed in Pubmed: [15734621](https://pubmed.ncbi.nlm.nih.gov/15734621/).
 13. Van de Veire NR, Schuijf JD, De Sutter J, et al. Non-invasive visualization of the cardiac venous system in coronary artery disease patients using 64-slice computed tomography. *J Am Coll Cardiol*. 2006; 48(9): 1832–1838, doi: [10.1016/j.jacc.2006.07.042](https://doi.org/10.1016/j.jacc.2006.07.042), indexed in Pubmed: [17084258](https://pubmed.ncbi.nlm.nih.gov/17084258/).
 14. Christiaens L, Ardilouze P, Ragot S, et al. Prospective evaluation of the anatomy of the coronary venous system using multidetector row computed tomography. *Int J Cardiol*. 2008; 126(2): 204–208, doi: [10.1016/j.ijcard.2007.03.128](https://doi.org/10.1016/j.ijcard.2007.03.128), indexed in Pubmed: [17493696](https://pubmed.ncbi.nlm.nih.gov/17493696/).
 15. Chen JJ, Lee WJ, Wang YC, et al. Morphologic and topologic characteristics of coronary venous system delineated by noninvasive multidetector computed tomography in chronic systolic heart failure patients. *J Card Fail*. 2007; 13(6): 482–488, doi: [10.1016/j.cardfail.2007.02.007](https://doi.org/10.1016/j.cardfail.2007.02.007), indexed in Pubmed: [17675063](https://pubmed.ncbi.nlm.nih.gov/17675063/).
 16. Młynarska A, Młynarski R, Kargul W, et al. Quality of visualization of coronary venous system in 64-slice computed tomography. *Cardiol J*. 2011; 18(2): 146–150, indexed in Pubmed: [21432820](https://pubmed.ncbi.nlm.nih.gov/21432820/).
 17. Młynarski R, Sosnowski M, Wlodyka A, et al. A user-friendly method of cardiac venous system visualization in 64-slice computed tomography. *Pacing Clin Electrophysiol*. 2009; 32(3): 323–329, doi: [10.1111/j.1540-8159.2008.02239.x](https://doi.org/10.1111/j.1540-8159.2008.02239.x), indexed in Pubmed: [19272061](https://pubmed.ncbi.nlm.nih.gov/19272061/).
 18. Młynarski R, Młynarska A, Tendera M, et al. Coronary sinus ostium: the key structure in the heart's anatomy from the electrophysiologist's point of view. *Heart Vessels*. 2011; 26(4): 449–456, doi: [10.1007/s00380-010-0075-3](https://doi.org/10.1007/s00380-010-0075-3), indexed in Pubmed: [21240507](https://pubmed.ncbi.nlm.nih.gov/21240507/).
 19. Parikh MG, Halleran SM, Bharati S, et al. Successful percutaneous cardiac resynchronization despite an occlusive Thebesian valve. *Pediatr Cardiol*. 2011; 32(8): 1223–1227, doi: [10.1007/s00246-011-0066-x](https://doi.org/10.1007/s00246-011-0066-x), indexed in Pubmed: [21805325](https://pubmed.ncbi.nlm.nih.gov/21805325/).
 20. Holda MK, Koziej M, Klimek-Piotrowska W. Thebesian valve: the cause of unsuccessful retrograde coronary sinus cannulation. *Anatol J Cardiol*. 2015; 15(3): E8–E9, doi: [10.5152/akd.2015.5952](https://doi.org/10.5152/akd.2015.5952), indexed in Pubmed: [25880190](https://pubmed.ncbi.nlm.nih.gov/25880190/).
 21. Noheria A, DeSimone CV, Lachman N, et al. Anatomy of the coronary sinus and epicardial coronary venous system in 620 hearts: an electrophysiology perspective. *J Cardiovasc Electrophysiol*. 2013; 24(1): 1–6, doi: [10.1111/j.1540-8167.2012.02443.x](https://doi.org/10.1111/j.1540-8167.2012.02443.x), indexed in Pubmed: [23066703](https://pubmed.ncbi.nlm.nih.gov/23066703/).
 22. Mahmoud HM, Al-Ghamdi MA, Ghabashi AE. Real time three-dimensional transesophageal echocardiography guided coronary sinus cannulation during CARILLON mitral annuloplasty device therapy for a patient with chronic severe mitral regurgitation. *Echocardiography*. 2015; 32(1): 181–183, doi: [10.1111/echo.12745](https://doi.org/10.1111/echo.12745), indexed in Pubmed: [25231878](https://pubmed.ncbi.nlm.nih.gov/25231878/).
 23. Strohmer B. Valve of Vieussens: an obstacle for left ventricular lead placement. *Can J Cardiol*. 2008; 24(9): e63, doi: [10.1016/s0828-282x\(08\)70676-7](https://doi.org/10.1016/s0828-282x(08)70676-7), indexed in Pubmed: [18787728](https://pubmed.ncbi.nlm.nih.gov/18787728/).
 24. de Oliveira IM, Scanavacca MI, Correia AT, et al. Anatomic relations of the Marshall vein: importance for catheterization of the coronary sinus in ablation procedures. *Europace*. 2007; 9(10): 915–919, doi: [10.1093/europace/eum175](https://doi.org/10.1093/europace/eum175), indexed in Pubmed: [17728261](https://pubmed.ncbi.nlm.nih.gov/17728261/).
 25. Hasdemir C, Alp A, Can LH. Successful balloon dilatation of the valve of Vieussens for left ventricular lead placement. *Pacing Clin Electrophysiol*. 2009; 32(6): 828–829, doi: [10.1111/j.1540-8159.2009.02376.x](https://doi.org/10.1111/j.1540-8159.2009.02376.x), indexed in Pubmed: [19545352](https://pubmed.ncbi.nlm.nih.gov/19545352/).

Cite this article as: Młynarski R, Młynarska A, Gołba KS, et al. Three-dimensional visualisation of coronary sinus ostium from the inside right atrium perspective. *Kardiologia Polska*. 2018; 77(3): 536–541, doi: [10.5603/KPa2017.0246](https://doi.org/10.5603/KPa2017.0246).